

# CHAPTER 5

## Product distributions and optimization study using response surface methodology

### 5.1 Introduction

The rapid increase in world's population along with the advancement in their living standard has led to think for a sustainable energy resource so that the use of available fossil fuels can be minimized. Pyrolysis of biomass has proved to be one of the important thermochemical conversion process but the interaction among the process variables play a very important role in deciding the desired product. Thus, statistical optimization of process variables for the yield of products is very essential.

RSM is a statistical tool to examine the interaction between the various independent process variables by performing the least number of experimental runs. The objective of RSM is to develop an experimental design for the analysis of responses and bring out the optimized condition. The different methods of RSM include Doehlert matrix, CCD and BBD (Kapur et al., 2016). BBD to some extent is more efficient than any other methods (Ferreira et al., 2007) since very few combinations of variables used for the determination of the response function (Muthukumar et al., 2003). The suitability of the

model is confirmed by the desirability value, and a value nearer to 1 suggests the best-optimized condition.

Thus, this work aimed to examine the combined effect of temperature, nitrogen flow rate and packed bed height on pyrolysis products distribution as well as maximizes the bio-oil and minimizes the biochar yield from SS using RSM based on BBD. Bio-oil collected at optimum condition was characterized for its physical (pH, density, HHV, viscosity, etc.) and chemical (FTIR and GCMS) properties. Biochar was characterized with proximate and ultimate analysis, HHV, BET surface area, SEM-EDX and FTIR.

## **5.2 Experimental**

### **5.2.1 Raw material**

Raw material collection and its preparation has been discussed in section 3.2.1.

### **5.2.2 Experimental setup and procedure**

Experimental set-up and pyrolysis process description has been discussed in section 4.2.3. Total seventeen (17) pyrolysis experimental runs were performed with the conditions produced by design expert statistical software, where three process parameters, temperature (500-700 °C), packed bed height (4-8 cm) and nitrogen flow rate (150-250 mL/min) were selected. During the experiment, heating of SS started from ambient temperature to the desired pyrolysis temperature. The system was maintained for 60 min at its final temperature, and then the heating was stopped. Cooling of the reactor was done in the continuous flow of nitrogen and once cooled, solid residue, i.e. biochar was collected from the reactor and taken for characterization. The liquid product was received from the flasks connected in series. It was further centrifuged and was separated from water by decantation using separating funnel. All the experiments were performed in triplicate, and the average value has been reported.

The equations for yield of biochar, bio-oil and pyrolytic gas have already been discussed in section 4.2.2.

### **5.2.3 Analytical instruments and methods used for characterization**

The analytical instruments and methods used for the characterization of bio-oil and biochar were similar as described in section 4.2.4.

### **5.2.4 RSM study**

The RSM is a regression method with a collection of mathematical and statistical techniques for the optimization of any process and finding the relationship between the independent variables and its responses (Mohammed et al., 2017). In the present study, Design Expert software was used for the optimization of maximum bio-oil yield and minimum biochar yield by employing BBD in RSM. The advantage of using RSM is that it reduces the number of experimental runs and gives more appropriate results. Three significant parameters that influence the pyrolysis process namely temperature (A), nitrogen flow rate (B) and packed bed height (C) were varied. All the parameters were utilized up to 3 levels 3 factors to enumerate the quadratic model with 5 centre points. The 3 factors in BBD are high (+1), low (-1) and center (0). The number of experiments in a BBD is given by  $N = k^2 + k + r$ , where  $k$  is the factor number and  $r$  is the repeated number of the centre point. Table 5.1 represents the experimental parameters and different BBD level. BBD provided total 17 experimental runs categorizing to 12 unique runs and 5 centre runs to assess the effect of process variables on bio-oil and biochar yield. Following that, results were evaluated using analysis of variance (ANOVA), co-efficient of determination ( $R^2$ ) and three-dimensional plots. The F and p values were obtained from the ANOVA analysis, where F-value indicates that the variation in the responses can be illustrated by the regression equation and p-value indicate whether F-value is large enough to assure statistical significance. A low p-value

(< 0.05) provides strong evidence that the given model is statistically significant (Dhanavath et al., 2017). The p-value for the lack of fit test was supposed to be insignificant (p-value > 0.05) for the model fitted. Adeq precision measures noise to signal ratio and are desirable for the model if it is greater than 4. The R-square, Adj R-square and Pred R-square values were analyzed for the optimization of process parameters. 3-D response plots were obtained based on the interaction between the three parameters and were studied. A non-linear second order regression model was used for fitting the experimental data and finds the coefficients of the equation. In the quadratic equation linear terms, square terms and linear-linear interaction terms were considered, and it could be described as:

$$Y = \alpha_0 + \sum \alpha_i X_i + \sum \alpha_{ii} X_i^2 + \sum \alpha_{ij} X_i X_j \quad (5.1)$$

Where, Y is the response (percentage of bio-oil and biochar yield),  $\alpha_0$  is the constant regression co-efficient,  $\alpha_i$ ,  $\alpha_{ii}$  and  $\alpha_{ij}$  are the coefficients for linear, quadratic and interaction effects (Charusiri and Numcharoenpinji, 2017; Ates and Ernigel, 2016).  $X_i$  and  $X_j$  represent coded independent parameters.

**Table 5.1 Range of independent process variables and experimental levels**

| Process variables           | Experiment levels |     |     |
|-----------------------------|-------------------|-----|-----|
|                             | -1                | 0   | 1   |
| Temperature (°C)            | 500               | 600 | 700 |
| Nitrogen flow rate (mL/min) | 150               | 200 | 250 |
| Packed bed height (cm)      | 4                 | 6   | 8   |

## 5.3 Results and Discussions

### 5.3.1 Physicochemical properties of SS

The physicochemical characteristics of SS are already discussed in section 3.3.1.

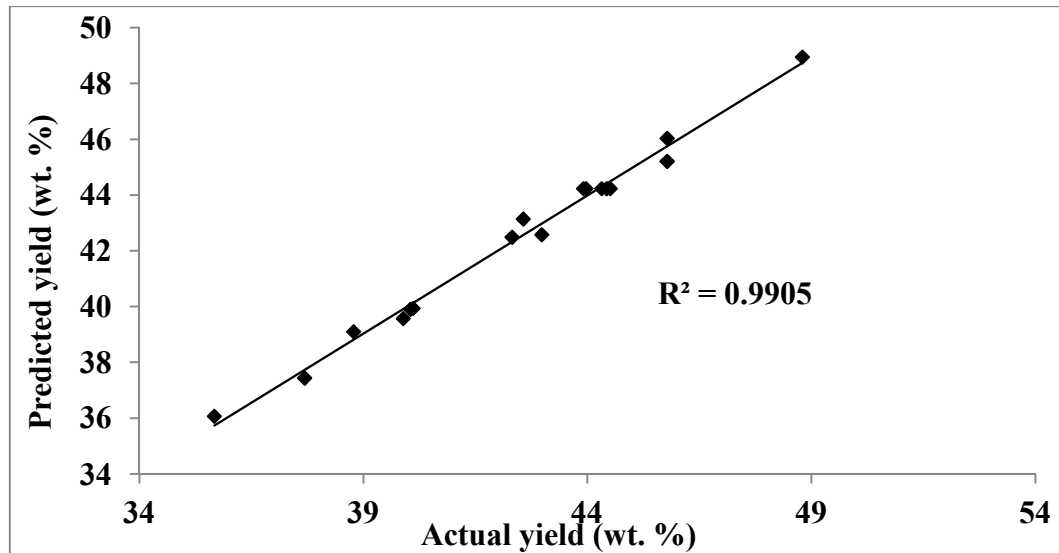
### 5.3.2 Box-Behnken design and statistical analysis

State-Ease Design Expert software was employed for the design and statistical study of the pyrolysis process. The BBD design was applied to the experimental results with 3 independent variables (temperature, nitrogen flow rate and packed bed height) at 3 levels (1, 0 and 1) to develop an experimental design.

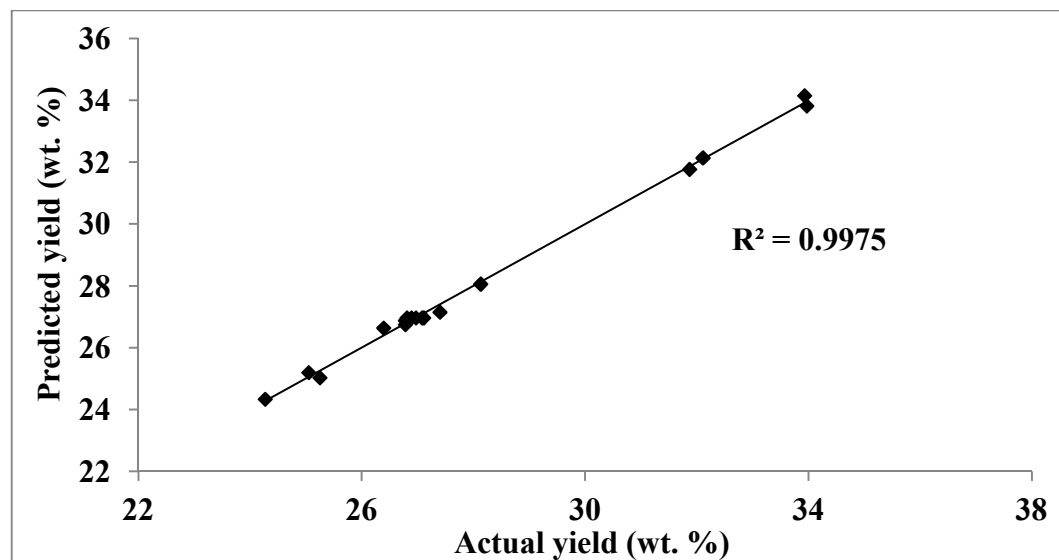
Based on the experimental conditions provided by the software, total 17 experiments (including 5 centre runs) were performed combining three process parameters to optimize the temperature of the process, nitrogen flow rate and packed bed height as presented in Table 5.2. Maximization of bio-oil and minimization of biochar yield was considered as the analyses response of the process. A regression analysis was done to find out the link between the dependent variable (responses) and independent variables (process variables). Fig. 5.1 (a) and (b) illustrates the graphical representation of actual (experimental) vs predicted (mathematically calculated) yield of bio-oil and biochar. The predicted and actual yields in both cases are very close to each other and deviation in the result is almost negligible as co-efficient of determination ( $R^2$ ) in both the cases is close to 1. The result suggests a strong relation between predicted model and its actual result and thus model can be used to predict the yield of bio-oil and biochar.

Table 5.2 Box-Behnken experimental design matrix and results

| Run | Temperature (°C) | Nitrogen flow rate (mL/min) | Packed bed height (cm) | Bio-oil yield (wt. %) |              | Bio-char yield (wt. %) |              |
|-----|------------------|-----------------------------|------------------------|-----------------------|--------------|------------------------|--------------|
|     |                  |                             |                        | Predicted             | Experimental | Predicted              | Experimental |
| 1   | 600.00           | 200.00                      | 6.00                   | 44.23                 | 43.91        | 26.97                  | 27.11        |
| 2   | 600.00           | 200.00                      | 6.00                   | 44.23                 | 44.51        | 26.97                  | 26.89        |
| 3   | 600.00           | 250.00                      | 4.00                   | 39.90                 | 40.05        | 26.64                  | 26.39        |
| 4   | 500.00           | 150.00                      | 6.00                   | 39.57                 | 39.89        | 34.15                  | 33.93        |
| 5   | 600.00           | 150.00                      | 4.00                   | 43.14                 | 42.57        | 28.06                  | 28.13        |
| 6   | 700.00           | 200.00                      | 8.00                   | 46.03                 | 45.78        | 25.20                  | 25.05        |
| 7   | 700.00           | 200.00                      | 4.00                   | 39.94                 | 40.11        | 26.88                  | 26.78        |
| 8   | 600.00           | 200.00                      | 6.00                   | 44.23                 | 43.97        | 26.97                  | 27.08        |
| 9   | 600.00           | 250.00                      | 8.00                   | 45.21                 | 45.78        | 24.34                  | 24.27        |
| 10  | 500.00           | 200.00                      | 8.00                   | 42.49                 | 42.32        | 32.14                  | 32.11        |
| 11  | 500.00           | 200.00                      | 4.00                   | 37.44                 | 37.69        | 33.82                  | 33.97        |
| 12  | 600.00           | 150.00                      | 8.00                   | 48.95                 | 48.80        | 27.15                  | 27.40        |
| 13  | 500.00           | 250.00                      | 6.00                   | 36.07                 | 35.67        | 31.77                  | 31.87        |
| 14  | 700.00           | 250.00                      | 6.00                   | 39.10                 | 38.78        | 25.03                  | 25.25        |
| 15  | 600.00           | 200.00                      | 6.00                   | 44.23                 | 44.43        | 26.97                  | 26.97        |
| 16  | 700.00           | 150.00                      | 6.00                   | 42.58                 | 42.98        | 26.75                  | 26.78        |
| 17  | 600.00           | 200.00                      | 6.00                   | 44.23                 | 44.32        | 26.97                  | 26.81        |



(a)



(b)

Fig. 5.1 Actual vs predicted yield of the model for (a) bio-oil and (b) biochar

### 5.3.3 ANOVA analysis

ANOVA was performed for the investigation of both, bio-oil and biochar yield by scrutinizing the quadratic model in BBD. Results of the ANOVA for the response of bio-oil and biochar yield are summarized in Tables 5.3 and 5.4, respectively. The approval of any quadratic model depends on the Fischer test value (F-value) and

probability value (p-value). A higher F-value describes the greater reliability of the model whereas lower p-value indicates the higher significance of the model (Arvindekar and Laddha, 2016; Nizamuddin et al., 2016).

According to the ANOVA for bio-oil yield from SS pyrolysis, the model F-value and p-value (Prob > F) of 81.48 and <0.001 means that the model is significant. There is only 0.01% (very small) chance that this large model F-value might occur because of noise. The p-value < 0.0500 indicates the significant model terms. In present case, A, B, C, A<sup>2</sup>, B<sup>2</sup> and C<sup>2</sup> are the significant model terms. Lack of fit “F-value” is an additional vital feature for ANOVA analysis that describes the suitability of the established quadratic regression model and its higher value is undesirable. Lack of fit is supposed to be not significant for a good and perfect model fitting (Sumic et al., 2016). Lack of fit F-value of 6.27 and p > 0.0500 describes its insignificant behaviour. Equation 5.1 expresses the developed model for the predictive bio-oil yield in wt. %. Similarly, ANOVA analysis of biochar yield was done. The model F-value and p-value of 305.69 and < 0.0001 suggests the significant behaviour of the regression model. There is only a 0.01% chance that F-value will be so large and that too because of noise. In the present case, the significant model terms are A, B, C, BC and A<sup>2</sup>. Higher F-value of 6.32 and p > 0.05 of “Lack of fit” implies insignificant behaviour of the model. Insignificant lack of fit indicates the suitability of the model. The model developed for the predictive biochar yield in wt. % is presented through equation 4.2.

$$\begin{aligned} \text{Bio-oil yield (wt. \%)} = & 44.23 + 1.51 A - 1.74 B + 2.78 C + 5.000E-003 AB + 0.26 AC \\ & - 0.12 BC - 3.86 A^2 - 1.04 B^2 + 1.11 C^2 \end{aligned} \quad (5.2)$$

$$\begin{aligned} \text{Biochar yield (wt. \%)} = & 26.97 - 3.50 A - 1.06 B - 0.81 C + 0.13 AB + 0.032 AC - \\ & 0.35 BC + 2.71 A^2 - 0.22 B^2 - 0.20 C^2 \end{aligned} \quad (5.3)$$



Where A, B and C represents the coded values of temperature, nitrogen flow rate and packed bed height. The positive and negative sign in the model equation indicates the synergic and antagonistic effects.

**Table 5.3 ANOVA analysis of bio-oil yield**

| Source                | Sum of squares | df | Mean square | F value    | p-value<br>Prob > F |                  |
|-----------------------|----------------|----|-------------|------------|---------------------|------------------|
| Model                 | 177.11         | 9  | 19.68       | 81.48      | <0.0001             | Signifi-<br>Cant |
| A-Temperature         | 18.24          | 1  | 18.24       | 75.53      | <0.0001             |                  |
| B-Nitrogen flow rate  | 24.36          | 1  | 24.36       | 100.87     | <0.0001             |                  |
| C - Packed bed height | 61.94          | 1  | 61.94       | 256.47     | <0.0001             |                  |
| AB                    | 1.000E-004     | 1  | 1.000E-004  | 4.141E-004 | 0.9843              |                  |
| AC                    | 0.27           | 1  | 0.27        | 1.12       | 0.3251              |                  |
| BC                    | 0.063          | 1  | 0.063       | 0.26       | 0.6266              |                  |
| A <sup>2</sup>        | 62.78          | 1  | 62.78       | 259.97     | <0.0001             |                  |
| B <sup>2</sup>        | 4.52           | 1  | 4.52        | 18.73      | 0.0034              |                  |
| C <sup>2</sup>        | 5.17           | 1  | 5.17        | 21.42      | 0.0024              |                  |
| Residual              | 1.69           | 7  | 0.24        |            |                     |                  |
| Lack of fit           | 1.39           | 3  | 0.46        | 6.27       | 0.0542              |                  |
| Pure error            | 0.30           | 4  | 0.074       |            |                     |                  |
| Cor total             | 178.80         | 16 |             |            |                     |                  |

**Table 5.4 ANOVA analysis of biochar yield**

| Source               | Sum of squares | df | Mean squares | F value | p-value<br>prob > F |             |
|----------------------|----------------|----|--------------|---------|---------------------|-------------|
| Model                | 143.74         | 9  | 15.97        | 305.69  | <0.0001             | Significant |
| A-Temperature        | 98.14          | 1  | 98.14        | 1878.38 | <0.0001             |             |
| B-Nitrogen flow rate | 8.95           | 1  | 8.95         | 171.23  | <0.0001             |             |
| C-Packed bed height  | 5.18           | 1  | 5.18         | 99.22   | <0.0001             |             |
| AB                   | 0.070          | 1  | 0.070        | 1.34    | 0.2843              |             |
| AC                   | 4.225E - 003   | 1  | 4.225E-003   | 0.081   | 0.7844              |             |
| BC                   | 0.48           | 1  | 0.48         | 9.25    | 0.0188              |             |
| A <sup>2</sup>       | 30.87          | 1  | 30.87        | 590.87  | <0.0001             |             |
| B <sup>2</sup>       | 0.21           | 1  | 0.21         | 3.98    | 0.0862              |             |
| C <sup>2</sup>       | 0.17           | 1  | 0.17         | 3.30    | 0.1123              |             |
| Residual             | 0.37           | 7  | 0.052        |         |                     |             |
| Lack of fit          | 0.30           | 3  | 0.10         | 6.32    | 0.0534              |             |
| Pure error           | 0.064          | 4  | 0.016        |         |                     |             |
| Cor total            | 144.11         | 16 |              |         |                     |             |

Table 5.5 depicts the model summary statistics of bio-oil and biochar yield. The standard deviations for bio-oil and biochar yield were 0.49 and 0.23, respectively. A very minute standard deviation (SD) is satisfactory, and it signifies excellent model fitting for the optimization. Mean responses for the bio-oil and biochar yield were 42.44 and 28.05 wt. %, respectively. Co-efficient of variation measures the relative SD of the experiment and presents the error in the form of mean percentage. In the present study,

the C.V. % for both bio-oil and biochar yield was 1.16 and 0.81%, respectively. A low C.V. % (< 10%) describes higher reliability and good reproducibility of the regression model (Mohammed et al., 2017). The co-efficient of variation ( $R^2$ ) for bio-oil and biochar yield were 0.9905 and 0.9975 which is very close to 1 satisfying good model fitting. Adjusted  $R^2$  and predicted  $R^2$  are the two other parameters that are considered in ANOVA analysis. Adjusted  $R^2$  improves the  $R^2$  by regulating the model terms where as predicted  $R^2$  suggests the deviation among the new data points explained by the regression model. For bio-oil and biochar yield the adjusted  $R^2$  value were 0.9748 and 0.9942 whereas predicted  $R^2$  were 0.8727 and 0.9658. The result suggests that the predicted  $R^2$  is in reasonable agreement with adjusted  $R^2$  values. Adequate precision deals with the noise to signal ratio and its value more than 4 is desirable. The bio-oil and biochar yield had the adequate precision of 34.179 and 55.972, respectively which indicates sufficient signal. Thus the above models are efficient to operate the design space.

**Table 5.5 Model summary statistics for bio-oil and biochar yield**

| Final products | Standard deviation | Mean  | C.V. (%) | $R^2$  | Adjusted $R^2$ | Predicted $R^2$ | Adequate precision |
|----------------|--------------------|-------|----------|--------|----------------|-----------------|--------------------|
| Bio-oil        | 0.49               | 42.44 | 1.16     | 0.9905 | 0.9748         | 0.8727          | 34.179             |
| Biochar        | 0.23               | 28.05 | 0.81     | 0.9975 | 0.9942         | 0.9658          | 55.972             |

### 5.3.4 Optimization and 3D-plots

To optimize the process parameters, numerical optimization study was carried out. The goal was to find the optimal condition that will maximize the bio-oil yield and minimize

the biochar yield keeping the process parameters (temperature, nitrogen flow rate and packed bed height) in range of the experimental conditions. However, to find out the effect of input parameters on response values and their interaction effect, three-dimensional surface plots were used. The RSM 3D plots for bio-oil and biochar yields are presented by varying two parameters and keeping the third parameter at constant as shown in Fig. 5.2, 5.3 and 5.4, respectively.

#### **5.3.4.1 Optimization of nitrogen flow rate and temperature**

The surface plot for the optimization of the nitrogen flow rate and the temperature is presented in Figs. 5.2 (a) and (b) for bio-oil and biochar yield, respectively. From the plot, it can be inferred that increase in temperature increased the bio-oil yield and reached to a maximum at optimum temperature whereas nitrogen flow rate showed reverse profile and bio-oil yield decreased with increasing flow rate of nitrogen. More volatiles are produced with an increase in temperature but beyond the optimum temperature lignin degradation and secondary reactions occur which produce more non-condensable gases decreasing the bio-oil yield (Soetardji et al., 2014).

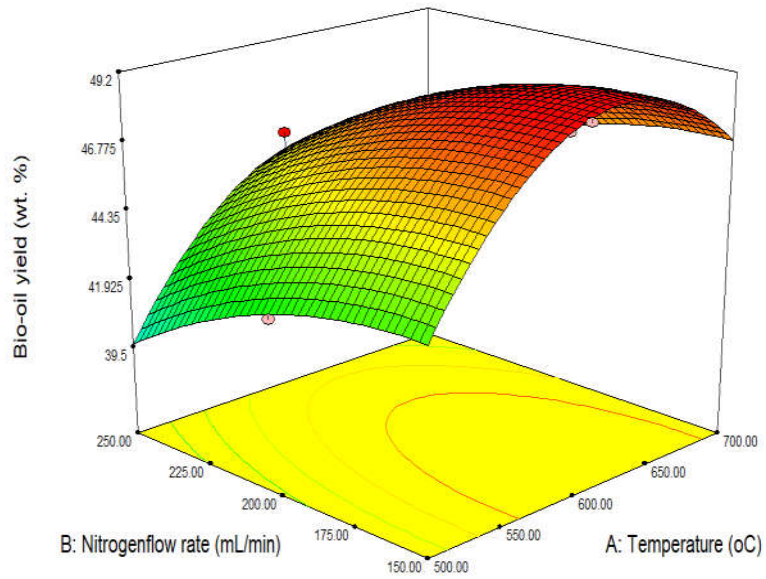
Higher nitrogen flow rate lowered the vapour residence time that leads to the escaping of uncondensed volatiles from the condenser and decreased the bio-oil yield. Impact of nitrogen flow rate and temperature on biochar yield is shown in Fig 5.2 (b). The interaction between these two parameters at constant packed bed height illustrated that temperature had an immense effect on biochar yield in comparison with nitrogen flow rate. A decreasing trend was observed in biochar yield with increasing temperature and nitrogen flow rate. This is due to more devolatilization of organic and lignocellulosic fractions with increasing temperature (Horne and Williams, 1996). The maximum bio-oil and minimum biochar yield were obtained at 639.45 °C and nitrogen flow rate of 181.59 mL/min at a constant packed bed height of 8 cm.

Design-Expert® Software

Bio-oil yield  
 48.8  
 35.67

X1 = A: Temperature  
 X2 = B: Nitrogen flow rate

Actual Factor  
 C: Packed bed height = 8.00



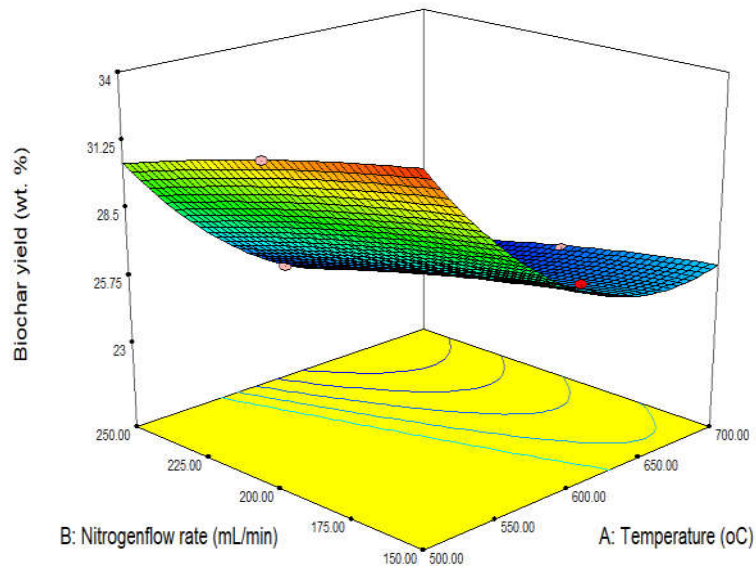
(a)

Design-Expert® Software

Biochar yield  
 33.97  
 24.27

X1 = A: Temperature  
 X2 = B: Nitrogen flow rate

Actual Factor  
 C: Packed bed height = 8.00



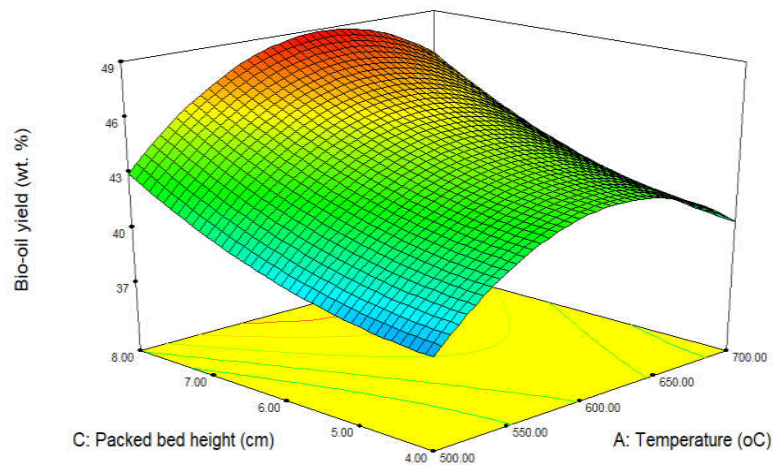
(b)

**Fig. 5.2 3-D surface response showing effects of temperature and nitrogen flow rate on (a) bio-oil and (b) biochar yield**

### 5.3.4.2 Optimization of temperature and packed bed height

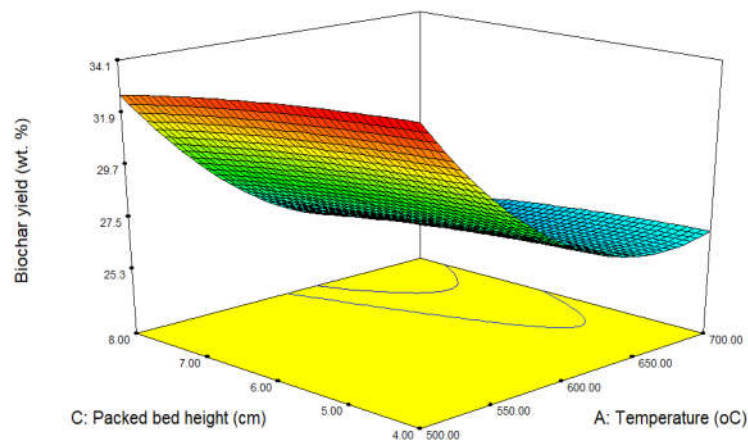
The surface plot for the optimization of temperature and packed bed height is shown in Fig. 5.3 (a) and (b). The results affirmed that maximum bio-oil and minimum biochar yield was attained at 639.45 °C and packed bed height of 8 cm in the continuous flow of

Design-Expert® Software  
Bio-oil yield  
48.8  
35.67  
X1 = A: Temperature  
X2 = C: Packed bed height  
Actual Factor  
B: Nitrogen flow rate = 181.59



(a)

Design-Expert® Software  
Biochar yield  
33.97  
24.27  
X1 = A: Temperature  
X2 = C: Packed bed height  
Actual Factor  
B: Nitrogen flow rate = 181.59



(b)

**Fig. 5.3 3-D surface response showing effects of temperature and packed bed height on (a) bio-oil and (b) biochar yield**

nitrogen at 181.59 mL/min. Higher packed bed height results to denser biomass bed which gives longer vapour residence time causing secondary cracking reactions to occur and form more volatiles and less biochar. Higher packed bed height and moderate temperature in continuous nitrogen purging were sufficient to convert sawdust to bio-oil and biochar.

#### **5.3.4.3 Optimization of nitrogen flow rate and packed bed height**

The surface response of bio-oil and biochar yield under the continuous flow nitrogen (150-250 mL/min) and packed bed height from 4 to 8 cm at 639.45 °C is depicted in Fig. 5.4 (a) and (b). The plots assured that bio-oil yield increased with the increasing packed bed height, but higher nitrogen flow decreased the yield. A higher nitrogen flow rate reduces the vapour residence time causing a decrease in the bio-oil yield whereas higher packed bed height caused a more secondary reaction that converts primary organic vapour into more volatiles and less biochar. The maximum bio-oil and minimum biochar yield were recorded at packed bed height of 8 cm and nitrogen flow rate of 181.59 mL/min at a constant temperature of 639.45 °C.

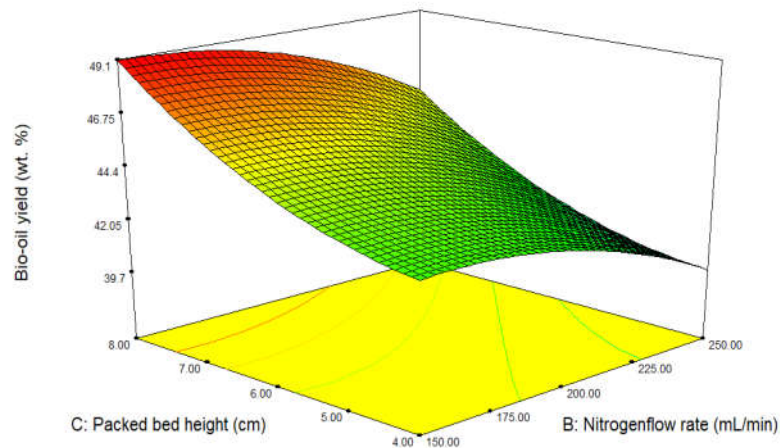
Design-Expert® Software

Bio-oil yield

48.8  
35.67X1 = B: Nitrogen flow rate  
X2 = C: Packed bed height

Actual Factor

A: Temperature = 639.45



(a)

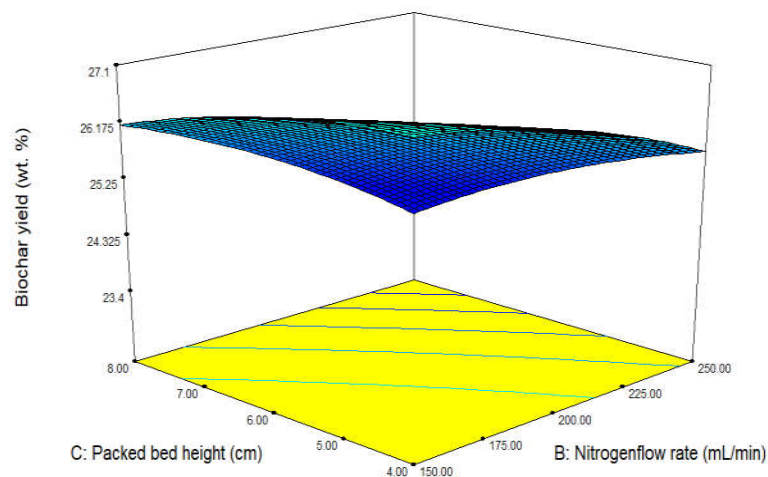
Design-Expert® Software

Biochar yield

33.97  
24.27X1 = B: Nitrogen flow rate  
X2 = C: Packed bed height

Actual Factor

A: Temperature = 639.45



(b)

**Fig. 5.4 3-D surface response showing effects of temperature and nitrogen flow rate on (a) bio-oil and (b) biochar yield**

#### 5.3.4.4 Validation of optimum result

For maximum bio-oil and minimum the biochar yield, process parameters were optimized where temperature, nitrogen flow rate and packed bed height were kept within the experimental conditions. The predicted result showed that temperature 639.45 °C, nitrogen flow rate around 181.59 mL/min and a packed bed height of 8 cm



was sufficient for optimum bio-oil production with the highest desirability of 0.949. To validate the results, pyrolysis experiments were performed at optimized conditions. The experiments were performed in triplicate, and the comparative (predicted and experimental) result is summarized in Table 5.6. The average bio-oil and biochar collected were 48.71 and 25.56, respectively. The deviation between the experimental and predicted results from the model is very less suggesting the adequacy of the model for maximum bio-oil and minimum biochar production.

**Table 5.6 Predicted and experimental yield at optimized condition**

| Parameters          |   |                              | Yield of<br>bio-oil<br>(wt. %) | Yield of<br>biochar<br>(wt. %) |              |
|---------------------|---|------------------------------|--------------------------------|--------------------------------|--------------|
| Temperature<br>(°C) | N <sub>2</sub> flow<br>rate<br>(mL/min) | Packed bed<br>height<br>(cm) |                                |                                |              |
| 639.45              | 181.59                                  | 8                            | 48.76                          | 25.49                          | Predicted    |
| 640                 | 180                                     | 8                            | 48.71                          | 25.56                          | Experimental |

### 5.3.5 Characterization of products

#### 5.3.5.1 Biochar characterization

The physicochemical properties of SS biochar produced at optimum pyrolysis condition are presented in Table 5.7. The VM was reduced to 11.45 wt. % whereas FC and AC was increased to 74.68 and 12.00 wt. %, respectively after pyrolysis suggesting highly carbonaceous nature of biochar. The increase in temperature leads to the devolatilization of SS and releasing more of the volatiles. The increase in the AC of biochar was due to the agglomeration of the inorganic nutrients but it is much lower in comparison to Indian fossil coals (Anupam et al., 2016). The high amount of FC with low VM and AC signifies good fuel properties of biochar. The ultimate analysis results revealed the increase in carbon content (C) whereas a decrease in oxygen (O) and hydrogen (H)

content. Higher carbon content can be utilized in the making of electrodes. In addition to it, it enhances the rate of carbon sequestration in the soil and also improves the soil

**Table 5.7 Physicochemical properties of biochar at optimized condition**

| <b>Proximate analysis (wt. %)</b>            |          |
|--|----------|
| MC   | 1.87     |
| VM   | 11.45    |
| AC   | 12.00    |
| FC*  | 74.68    |
| FC/(VM+FC)                                   | 0.87     |
| <b>Ultimate analysis (wt. %)</b>             |          |
| C  | 80.07    |
| H  | 2.32     |
| N  | 1.33     |
| O*   | 16.28    |
| S  | Bdr      |
| H/C  | 0.35     |
| O/C  | 0.15     |
| <b>HHV (MJ/kg)</b>                           | 28.54    |
| <b>BET surface area (m<sup>2</sup>/g)</b>    | 281.8140 |
| t-plot micropore volume (cm <sup>3</sup> /g) | 0.122443 |
| BJH adsorption average pore diameter (nm)    | 3.0339   |
| BJH desorption average pore diameter (nm)    | 2.6255   |

\*- by difference, bdr - below detection range

quality by lowering the nutrients decomposition rate (Tripathi et al., 2016). Low H/C and O/C molar ratio indicate a higher degree of carbonization and greater stability of the biochar. It also confirms good quality of fuel as it leads to less energy loss and low smoke emission (Liu et al., 2013). Thermal stability of biochar is also confirmed by FC/(VM / FC) and O/C ratios. FC/(VM / FC) ratio of 0.87 was calculated in this study and indicating its thermal stability, and O/C ratio of less than 0.2 signified the biochar life of more than 1000 years (Spokas, 2010). HHV of SS biochar is significantly high suggesting better solid fuel characteristics. EDX analysis marked the presence of important mineral nutrients (Na, Mg, Ca, K, etc.) needed for the plant growth and in soil amendment. Thus, SS biochar can be applied to the soil for better agricultural crop production. SEM image (Fig. 5.5) showed the structural deformations in the biochar. SS has rough and disorganized structures with very few pores whereas holes and craters were developed due to devolatilization after pyrolysis which enhanced the porous structure of biochar. The result was escorted by BET surface area analysis. Biochar had high BET surface area of 281.8140 m<sup>2</sup>/g and corresponding t-plot micropore volume was 0.122443 cm<sup>3</sup>/g. The BJH adsorption/desorption average pore diameter is 3.0339/2.6255 nm. Higher porosity and high surface area suggest its utility as an adsorbent in waste stream purification or as catalyst support (Ren et al., 2014).

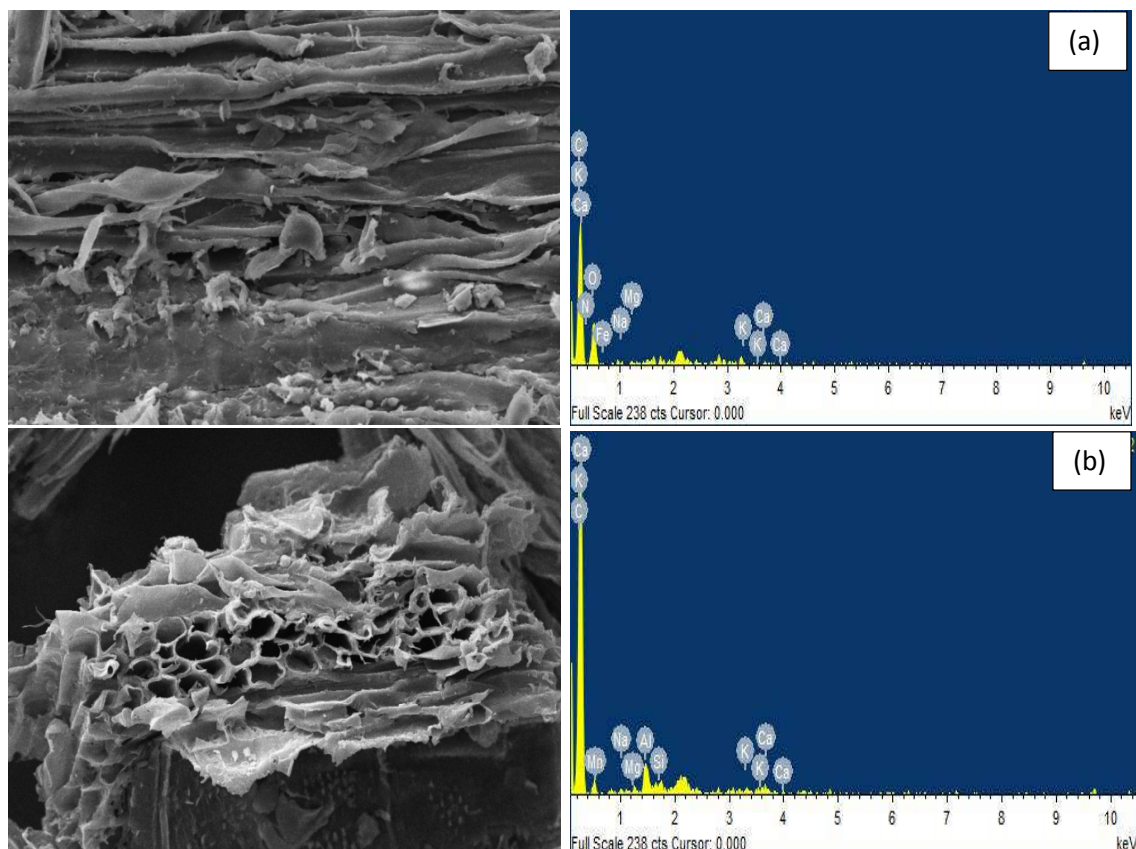


**Fig. 5.5 SEM-EDS of (a) SS and (b) biochar at optimized condition**

### 5.3.5.2 Physicochemical properties of bio-oil

Table 5.8 presents the physicochemical and fuel characteristics of produced bio-oil from SS pyrolysis at optimum condition and its comparison with the ASTM specifications. Bio-oil had the brownish appearance with very acrid smell. It had acidic characteristics with a corresponding pH value of 2.68. This low pH value attributes to the presence of various acidic compounds (acetic acids, carboxylic acids, etc.) and phenols that need to be treated before use as it is corrosive to aluminium, steel and nickel-based materials (Abnisa et al., 2011). Viscosity and density of the bio-oil describe its flow characteristics. Both the parameters are in the lower range as described by ASTM specifications. The Ramsbottom carbon residue explains the carbon forming tendency of the oil at high temperatures, and it came out to be 3.16 wt. %. The AC of the bio-oil

was 0.07 wt. % which is in the acceptable range. The HHV of the bio-oil describes the fuel characteristics, and it was 24.01 MJ/ kg. This high value indicates the existence of various carbon-rich organic compounds. Characteristics of Tunisian almond shell bio-oil at 473 °C studied by Grioui et al. (2014) had the pH value, density and calorific value of 3.1, 1.07 g/cm<sup>3</sup> and 27.40 MJ/kg, respectively. Similarly, Zhang et al. (2011) recorded the calorific value and density of peanut shell bio-oil to be 21.80 MJ/kg and 1.3 g/cm<sup>3</sup> at 500 °C. Thus, the results connote that bio-oil can be considered as both ASTM-Grade G and D. This slight difference in properties of the bio-oil produced from different biomass is due to its different chemical composition.

**Table 5.8 Physicochemical properties of bio-oil at optimum conditions compared with the ASTM D7544-12 specifications**

| Property                          | Bio-oil | ASTM-Grade G | ASTM-Grade D |
|-----------------------------------|---------|--------------|--------------|
| Appearance                        | Brown   | -            | -            |
| pH                                | 2.68    | Report       | Report       |
| Density (g/cm <sup>3</sup> )      | 1.092   | 1.1-1.3      | 1.1-1.3      |
| Viscosity (cSt)                   | 29.87   | 125 max      | 125 max      |
| Ramsbottom carbon residue (wt. %) | 3.16    | -            | -            |
| HHV (MJ/kg)                       | 24.01   | 15 min       | 15 min       |
| AC (wt. %)                        | 0.07    | 0.25 max     | 0.15 max     |

### 5.3.5.3 FTIR analysis of bio-oil

An FTIR spectrum confirms the presence of various chemical compounds in the bio-oil as depicted in Fig. 5.6. A large peak in the region of 3418 cm<sup>-1</sup> marks the presence of

compounds containing O-H group (Phenols and alcohols). The peak at  $2969.28\text{ cm}^{-1}$  corresponds to the C-H stretching vibrations of saturated hydrocarbons in the bio-oil (Guo et al., 2015). The peaks in between  $1639$  and  $1722\text{ cm}^{-1}$  attribute to the C=O bonds which indicate the existence of carboxylic acids, ketones and aldehydes in bio-oil. Presence of vibration around  $1516\text{ cm}^{-1}$  is ascribed to C=C in alkenes and benzene.

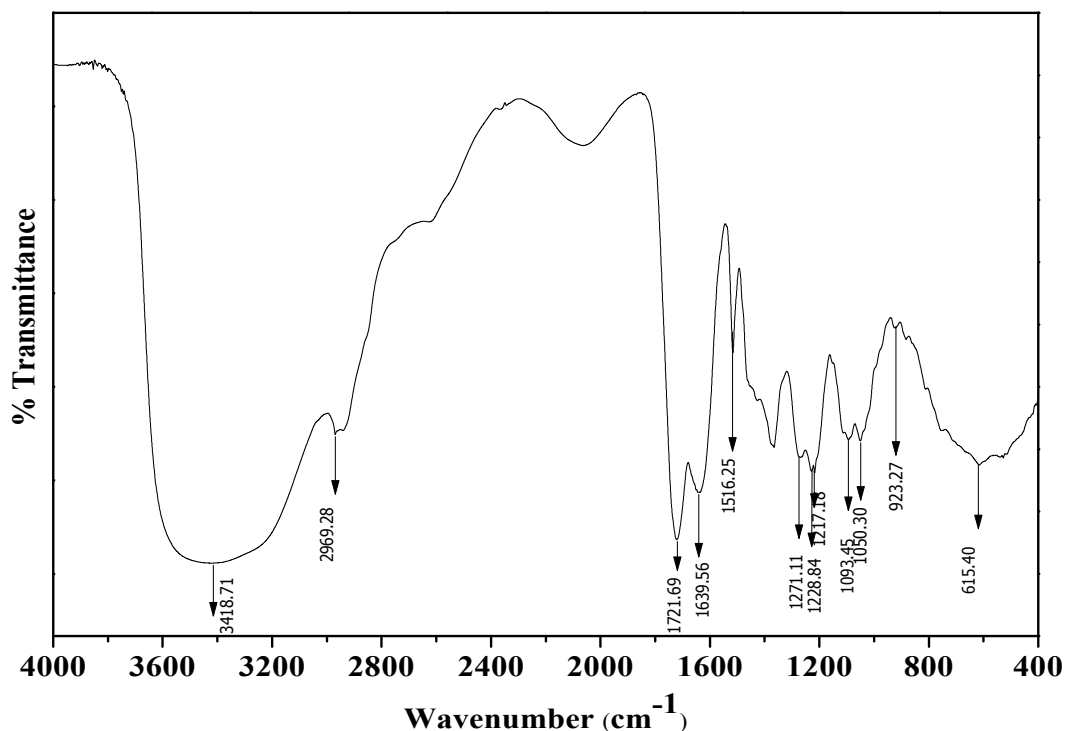


**Fig. 5.6 FTIR spectra of bio-oil at optimized condition**

Various peaks were observed in the wide range of  $1050$ - $1280\text{ cm}^{-1}$  which certifies the existence of C-O stretches of alcohols, esters and ethers. The peaks in the wave number range of  $610$ - $925\text{ cm}^{-1}$  the stretching vibrations of alkenes and alkynes. Thus the FTIR analysis suggests the presence of various valuable compounds and can be used as fuel after up gradation. However, detailed information about the compounds in bio-oil was achieved after GC-MS analysis.

#### 5.3.5.4 GC-MS analysis of bio-oil

Identification of specific chemical components in the bio-oil obtained from sawdust pyrolysis at optimized condition was done by GC-MS analysis and is presented in Table 5.9 and Fig. 5.7. The relative peaks of the GC-MS signify that bio-oil is a complex mixture containing various organic compounds and hydrocarbons like aliphatic, aromatics, phenols, alcohols, ketones, aldehydes, acids etc. which is in agreement with

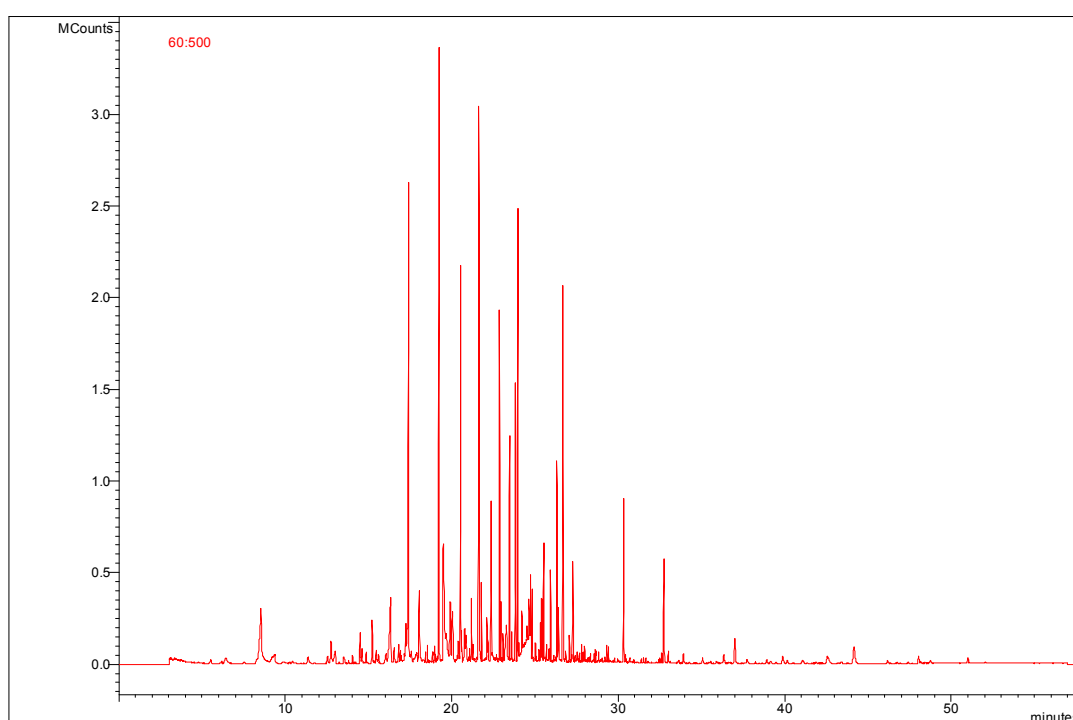


**Fig. 5.7 GC-MS analysis of bio-oil at optimized condition**

FTIR results (Lim et al., 2016). Aliphatic components in the bio-oil include alkanes, alkenes and their derivatives whereas benzene and phenol derivatives constitute the aromatic group. The dominant species in the bio-oil were oxygenated groups mainly phenolic, aldehydes, ketones and acids (phenol, 4 methoxy-2-methyl Phenol, 2 allyl-3,4dimethoxy phenol, 7 methyl-9,10 anthraquinones 1-carboxylic acid, ferulic acid, 2,2-

dimethyl cyclohexanone etc.). Other compounds recognized were a hydrocarbon (naphthalene-2-ethenyl, 1-1 diphenyl-2-methyl propane). Decomposition of cellulose and hemicellulose leads to the creation of carbonyls and carboxylic compounds during pyrolysis whereas breakage of aromatic rings and carbon-carbon scission in the lignin structure results to the formation of alkylphenols, phenols and its derivatives. Phenol and ketones constituted the major components in the bio-oil that can be further converted into liquid fuel and value-added chemicals. The greater amount of phenolic compounds in the bio-oil enhances the HHV of bio-oil (Nanda et al., 2014). The other components in the bio-oil can be up graded to increase its fuel value and lower the corrosiveness of the bio-oil by separating the oxygenated components for its use as boiler fuel. Also, bio-oil can be considered a source of valuable commercial chemicals like phenols, acids, ketones, benzene, etc.

**Table 5.9 GC-MS analysis of bio-oil at optimized condition**

| Sl. No. | Retention time (RT) | Compound                                 | Molecular formula                              | Area (%) |
|---------|---------------------|--|--|----------|
| 1       | 8.650               | 2-Octyn-1-ol                             | C <sub>8</sub> H <sub>14</sub> O               | 1.385    |
| 2       | 14.492              | 3,4-bis (hydroxymethyl) furan            | C <sub>6</sub> H <sub>8</sub> O <sub>3</sub>   | 0.812    |
| 3       | 14.600              | 3-(3'-butenyl) cyclohexanone             | C <sub>10</sub> H <sub>16</sub> O              | 0.309    |
| 4       | 15.216              | Phenol                                   | C <sub>6</sub> H <sub>6</sub> O                | 1.124    |
| 5       | 16.265              | 4-Methoxy (hydroxyl) methyl furan-2-one  | C <sub>6</sub> H <sub>8</sub> O <sub>4</sub>   | 1.671    |
| 6       | 17.232              | 2,3-Dimethyl-4-pyrone                    | C <sub>7</sub> H <sub>8</sub> O <sub>2</sub>   | 0.381    |
| 7       | 17.401              | 2,2-Dimethyl cyclohexanone               | C <sub>8</sub> H <sub>14</sub> O               | 9.738    |
| 8       | 18.047              | 4 methoxy-6-pentyl-5-6-dihdropyran-2-one | C <sub>11</sub> H <sub>18</sub> O <sub>3</sub> | 1.854    |



|    |        |   |  |        |
|----|--------|---|--|--------|
| 9  | 19.229 | 4 Methoxy-2-methyl Phenol   | C <sub>8</sub> H <sub>10</sub> O <sub>2</sub>  | 11.261 |
| 10 | 19.490 | Acetic acid, decyl ester  | C <sub>12</sub> H <sub>24</sub> O <sub>2</sub> | 3.611  |
| 11 | 20.530 | 4-Hexanoylresorcinol  | C <sub>12</sub> H <sub>16</sub> O <sub>3</sub> | 5.506  |
| 12 | 21.629 | Napthalene-2-ethenyl  | C <sub>12</sub> H <sub>10</sub>                | 11.437 |
| 13 | 22.113 | 1,3 Benzendiol-4-hexyl  | C <sub>12</sub> H <sub>18</sub> O <sub>2</sub> | 0.659  |
| 14 | 22.369 | exo Tricyclo [5,3,2,0(1,7)]dodecan-2-<br>ol   | C <sub>12</sub> H <sub>20</sub> O              | 2.902  |
| 15 | 22.868 | 1,1 Biphenyl-4-methyl   | C <sub>13</sub> H <sub>12</sub>                | 5.114  |
| 16 | 22.948 | 3 Allyl-6 methoxyphenyl acetate   | C <sub>12</sub> H <sub>14</sub> O <sub>3</sub> | 0.820  |
| 17 | 23.470 | 1,4, dimethoxy, 2,6,dimethyl benzene  | C <sub>10</sub> H <sub>14</sub> O <sub>2</sub> | 3.772  |
| 18 | 23.828 | 4-4 Dimethyl biphenol   | C <sub>14</sub> H <sub>14</sub>                | 4.750  |
| 19 | 23.966 | cis- Conferryl alcohol  | C <sub>10</sub> H <sub>12</sub> O <sub>3</sub> | 7.854  |
| 20 | 24.216 | 1-[4-hydroxy-3-[3,4,5-trihydroxy-6-<br>(hydroxymethyl)oxan-2-<br>yl]oxyphenyl] ethanone | C <sub>14</sub> H <sub>18</sub> O <sub>8</sub> | 0.503  |
| 21 | 24.748 | 2 Allyl-3,4dimethoxy phenol   | C <sub>11</sub> H <sub>14</sub> O <sub>3</sub> | 1.618  |
| 22 | 24.824 | Ferulic acid  | C <sub>10</sub> H <sub>10</sub> O <sub>4</sub> | 0.934  |
| 23 | 25.334 | Vanillyl ethyl ether  | C <sub>10</sub> H <sub>14</sub> O <sub>3</sub> | 0.518  |
| 24 | 25.406 | 4 Ethoxy-3 methoxyphenetyl alcohol  | C <sub>11</sub> H <sub>16</sub> O <sub>3</sub> | 1.330  |
| 25 | 25.523 | 3-H-4-Naptha [3,4b] Pyran   | C <sub>13</sub> H <sub>10</sub> O              | 1.929  |
| 26 | 25.936 | Cis-4-Propenyl syringol   | C <sub>11</sub> H <sub>14</sub> O <sub>3</sub> | 1.181  |
| 27 | 26.319 | 3 Phenyl acetophenone   | C <sub>14</sub> H <sub>12</sub> O              | 3.410  |
| 28 | 26.676 | 1-1 Diphenyl-2-methyl propane   | C <sub>16</sub> H <sub>18</sub>                | 6.750  |
| 29 | 27.275 | 4-Phenyl propiophenone  | C <sub>15</sub> H <sub>14</sub> O              | 2.226  |
| 30 | 30.327 | 7 Methyl-9,10 Anthraquinone 1-<br>carboxylic acid                                       | C <sub>16</sub> H <sub>10</sub> O <sub>4</sub> | 2.735  |
| 31 | 32.867 | Bis (2-hydroxy-4-<br>methoxyphenyl)methanone  | C <sub>15</sub> H <sub>14</sub> O <sub>4</sub> | 0.763  |

## **5.4 Conclusions**

The optimization of process parameters for pyrolysis of SS was investigated in this study. The optimum process condition to maximize bio-oil and minimize biochar yield concerning temperature, nitrogen flow rate and packed bed height were determined using BBD in RSM. A quadratic regression model was developed based on statistical analysis and optimum temperature of 640 C, nitrogen flow rate of 180 mL/min and sawdust packed bed height of 8 cm was obtained. The high F-value and low p-value (< 0.0001) in the ANOVA proved the yield of bio-oil and biochar as significant. The experimental yields of bio-oil and biochar at optimized conditions were in good agreement with the RSM predicted yields. Produced bio-oil was characterized with GC-MS, FTIR and physicochemical properties showing its applicability in engines after up gradation or as feedstock for valuable chemicals. Proximate and ultimate analysis exposed the high amount of carbon in biochar and HHV. BET and SEM analysis indicated the porous nature of biochar. Therefore, it can also be used as biocatalyst in a process industry or may be as good adsorbent for waste stream purification.

Based on RSM analysis, the biochar yield at optimized condition was used to remove Cr(VI) from aqueous solution for its applicability described in next chapter.